Ag Incorporated MoO_3 Thin Films and Fabrication of Ag/MoO_3/p-Si Structured Photodiode

G.Lavanya [1], N.Sivanandan [2*]

[1] *Research scholar, Department of Electronics, PSG College of Arts and Science, Coimbatore, Tamil Nadu, India.* lavanya.gnanavelk@gmail.com

[2] *Assistant Professor, Department of Electronics, PSG College of Arts and Science, Coimbatore, Tamil Nadu, India.* sivanandan@psgcas.ac.in

Abstract: MoO_3 have been widely investigated for their applications ranging from electronics to energy storage. Orthorhombic structured MoO_3 thin films were prepared on a glass substrate. The Ag doped materials to add the MoO_3 in different concentrations (1%, 3%, 5%) at Wt% with MoO_3 precursor and synthesis was done using the spray pyrolysis method. X-ray diffraction revealed the incorporation of Ag in the MoO_3 orthorhombic structure. FE-SEM images showed more dispersive and rod shapes than Agi-doped MoO_3 and pure MoO_3 respectively. The jet nebulizer spray pyrolysis technique for fabrication of n-Ag: MoO3/p-Si photodiodes makes it suitable for good response photo-detecting applications.

Keywords: MoO_3, orthorhombic structure, photodetector.

1. INTRODUCTION

Semiconductor nanostructures finds to be a powerful platform in the field of nanoscience today due to their versatile structures. Many transition metal oxides, such as MoO_3, WO_3, ZnO, CuO and NiO are widely used [1-5]. Among those materials, MoO_3 is a wide band gap n-type material which is used in many industrial applications because of its structural and electronic characteristics. Many authors had reported that the changes induced by substitution of transition metal ions into MoO_3 lattice [6-8]. However, among all, Ag doping into MoO_3 may manipulate the defect environment in the host material. In existing electronics field, the transition metal oxide (TMO) can be used in device fabrication as an n-type layer on the p-type silicon wafer for P–N junction diode structure. In fact, MoO_3 has been used in various applications of solar cell, diode, gas sensor, electrochromic, in fact that MoO3/Si material preparation of the photodiodes by ion-beam sputter technology and so on. Various deposition methods have been used to develop MoO_3 thin films such as spray pyrolysis, thermal vacuum evaporation, sol–gel, electron beam evaporation technique, hydrothermal, magnetron sputtering, laser coating, continuous wave CO_2 laser-assisted evaporation, oxygen plasma assisted molecular beam epitaxy, electrodeposition, chemical vapor deposition[9-12]. An attempt have been made for preparing uniform thin film using jet nebulizer spray pyrolysis technique. In the present work, a systematic attempt has been made to synthesize pure and Ag:MoO_3 nanoparticles (x=1, 3 and 5%) with different dopant concentrations by precipitation method. The influence of Ag doping on structural, morphological, optical and electrical properties of the synthesized samples were also investigated as well.

2. XRD ANALYSIS

Fig 1. Shows typical XRD pattern of prepared pure MoO_3, Ag doped MoO_3 with Ag. wt%: 1,3 and 5 samples calcination at 450°C using spray pyrolysis technique.. The position of diffraction peaks (1 0 1), (0 0 2), (0 1 1) depicts that it exhibits an orthorhombic crystal structure of MoO_3. These prominent peaks confirm the presence of orthorhombic phase of MoO_3 (α- MoO_3) in the prepared samples JCPDS no. 89-5108. When the Ag concentration increases, it is noted that the peak position in the XRD pattern shifts to higher 2θ values [13,14]. The higher 2θ peak position shift is due to occupancy of the MO^{6+} (Ionic Radius=0.56Å) which is smaller than Ag^{3+} (Ionic Radius =0.89Å) causing a few

kind of lattice distortion induced due to tensile stress, resulting a crystalline structure with extremely anisotropic growth of the oxide [15-17]

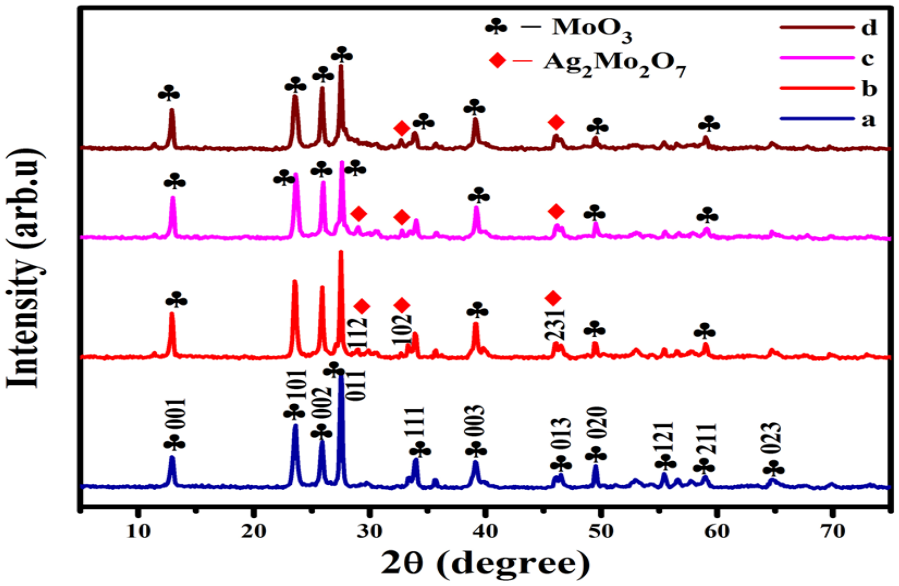

Fig 1. XRD pattern of Pure $MoO_3$and Ag doped MoO_3

Fig 2. Shows doping concentration of Ag with MoO_3. It is observed that the dislocation density is slightly increases with the increase of doping concentration. This is due to the decrease in grain size and the presence of improved defect states. It is noted that that the Ag doping lead to descent in the crystalline nature of the MoO_3. It is observed that the decrease in the lattice parameters seem to be relatively defensible as ionic radii of Ag^{3+} is higher than that of Mo^{6+}. The unit cell volume slightly increases and its micro strain decreases than that of pure MoO_3 which is due to the contamination of more supportive in non-equilibrium positions [18,19]. However , the unit cell volume seems to be decreases for 10 to 15% Ag^{3+} doping which may be due to mismatch between the radii of Ag^{3+} and Mo^{6+}.

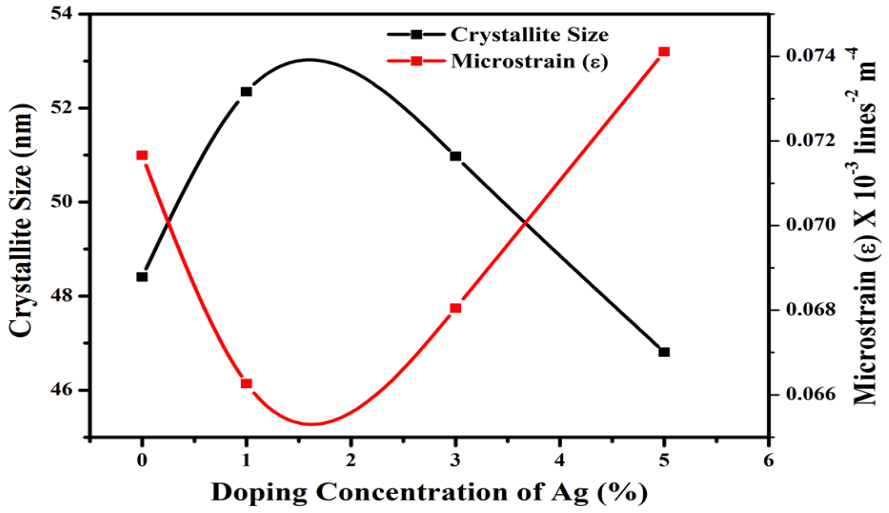

Fig 2. Doping concentration Ag of Crystallite size vs Microstrain

3. FE-SEM ANALYSIS

Fig 3 depicts the synthesized pure MoO_3 with 1%,3% and 5% Ag doped MoO_3 thin samples investigated by 2µm low magnification using FE-SEM examination. From the fig 3 a images of multi dispersive and ununiformed size rods are found with pure MoO_3. From the resulting images as depicted, it can be noted that the developed sample morphologies are having shape variation with loose surface tension with the increase in dopant concentration [20-22].

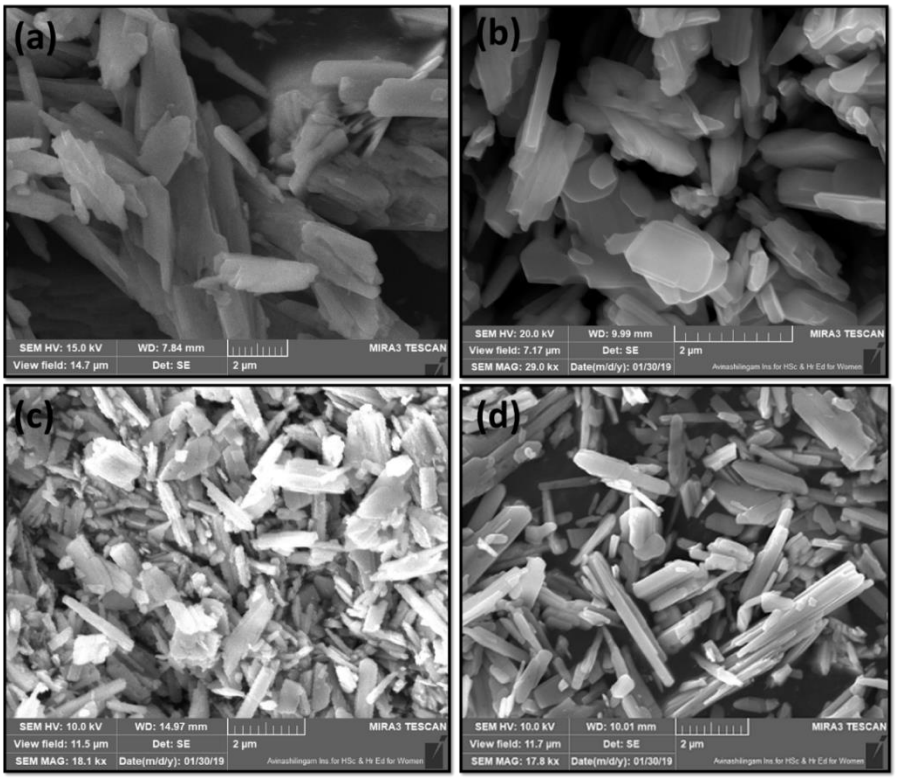

Fig 3. Morphology and microstructure of the pure and Ag doped MoO_3 thinfilms by FE-SEM.

4. EDS ANALYSIS

The constituents of the samples were quantitatively characterized by the measurement of EDS analysis. The EDS spectra of pure and Ag doped MoO_3 thinfilms are depicted in Fig. 4 (a-d).

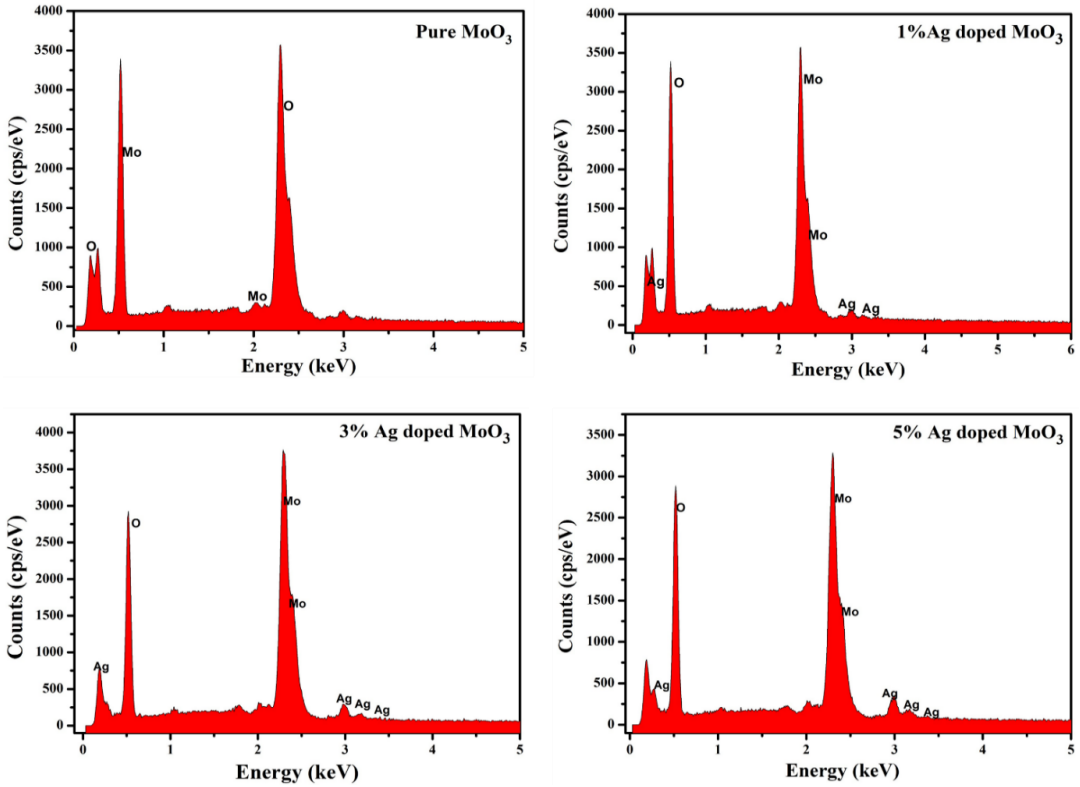

Fig 4. Elemental analysis of pure and Ag doped MoO_3 thinfilms

These spectra designate that presence of Molybdenum (Mo),Oxygen (O) and Silver (Ag) as the clearly well known that of the components, products and low concentration of Ag^{3+} ions along with elemental mapping. consequently, the EDS results says that the majority of the undesired precursor materials have been absolutely removed from the product.

Table 1. Elemental analysis of pure and Ag doped MoO_3 thinfilms

(a)

Elements	Weight %	Atomic %
O k	35.68	75.82
Mo L	64.32	24.18

(b)

Elements	Weight %	Atomic %
O k	36.65	78.92
Ag L	5.77	1.85
Mo L	57.58	19.23

(c)

Elements	Weight %	Atomic %
O k	28.54	70.85
Ag L	9.28	2.41
Mo L	62.18	26.74

(d)

Elements	Weight %	Atomic %
O k	26.02	68.40
Ag L	10.36	3.70
Mo L	63.62	27.90

5. I-V CHARACTERISTICS OF N-AG DOPED MOO_3/P-SI DIODES

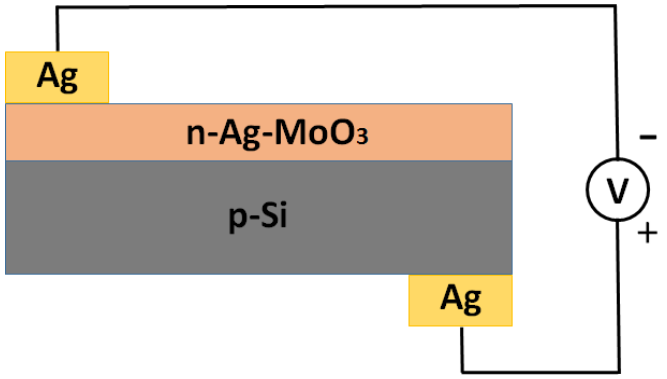

Fig. 5(a) The device structure of back contact

Fig.5 (a) shows represents the schematic of n-MoO_3/ p-Si device structure the current voltage characteristics of undoped and Ag (wt.5%) doped n-MoO_3/p-Si diode. The parameters of both devices were analyzed under illumination source of a halogen lamp and in darkness condition using I-V characteristics it exhibits asymmetrical and non-linear behavior as illustrated by figure (b – e) It is observed that the studied diodes, under dark condition exhibits the rectification behavior [23-26].

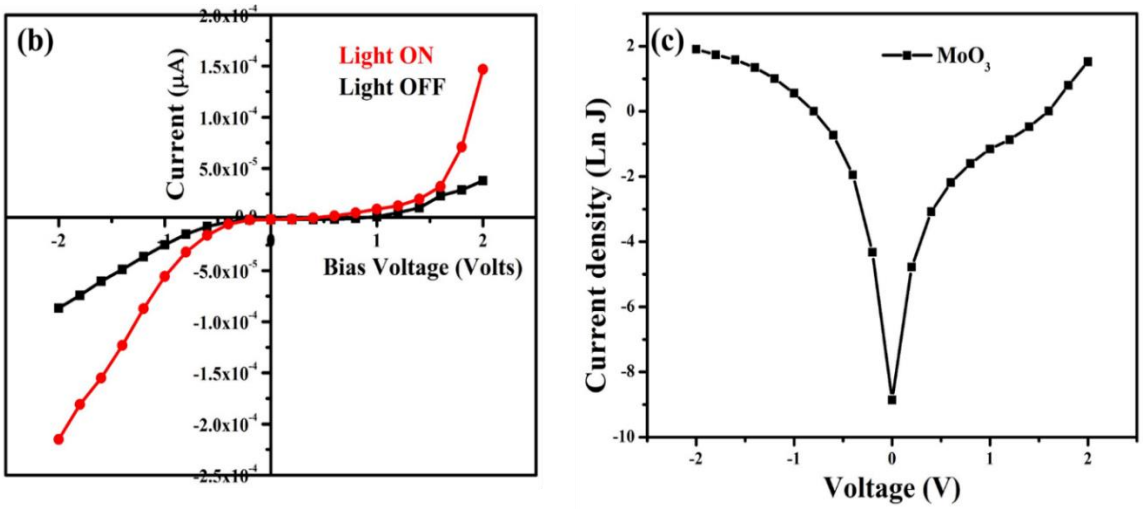

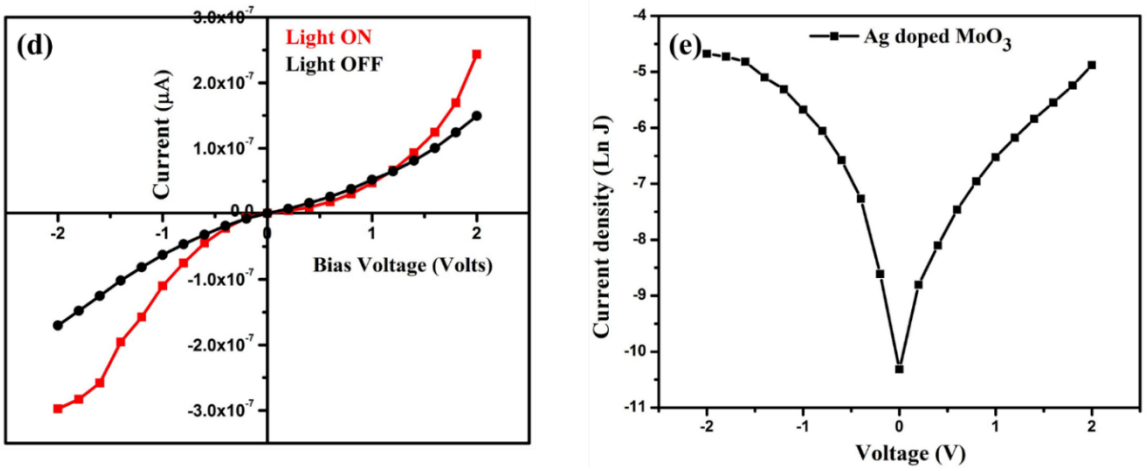

Fig. 5. (b-d). I-V curve of (b) n-MoO_3/p-Si, (d) n-Ag MoO_3/p-Si diodes, I-V curve of (c,e) current density (J)-voltage (V) plots of pure MoO_3 and n-Ag MoO_3/p-Si diodes

The thermionic emission current-voltage dependence of the junction of the applied voltage (V) may be written as the equation (1),

$$I = I_s\left[\exp\left(\frac{qV}{nKT}\right)-1\right]\left(V \geq 3k_B\, T/q\right) \text{----------(1)}$$

The rectification ratio is found to be dependent on the substitution of silver content. It is noted that RR decreases with increasing the dopant concentration.

The saturation current I_s is expressed by the equation (2)

$$I_s = AA^*T^2\exp\left(-\frac{q\Phi_B}{KT}\right) \text{----------(2)}$$

The ideality factor, n can be calculated from the slope straight line region during the forward bias ln (I)-V plot and can be written by the equation

$$n = \frac{q}{KT}\frac{dV}{d(\ln I)} \text{----------(3)}$$

where, I_o can be determined by extrapolation of the forward bias ln (I)-V curve to V=0. The Φ_B is calculated by the following relation

$$\Phi_B = \frac{KT}{q}\ln\left(\frac{AA^*T^2}{I_o}\right) \text{----------(4)}$$

Where I_0, q, V, n, KB, T and A^* is the reverse leakage current density, electron charge, applied voltage, ideality factor, Boltzmann constant, temperature in K and effective Richardson constant for p-type Si wafer. The ideality factor was determined form the slop of the intercept of the semi-logarithmic forward biased J-V plot. The ideality factor (n) and barrier height (ΦB) values for MoO3 and Ag doped MoO_3 were calculated in the values are given Table 2.

Table 2 Electrical parameters of the MoO_3 diode

sample	Ideality factor (n)	Barrier height (Φ_B)	Saturation current (Io)
MoO_3	1.4855	0.40972	5.41×10^{-5}
Ag 5% doped MoO_3	4.0975	0.57694	8.95×10^{-8}

The ideality factor (n) and barrier height (ΦB) values for MoO3 and Ag doped MoO_3 for the dark and light illumination condition has been studied and the ideality factor is found to be increasing whereas the barrier height of the device is found to be increased for the same condition. It is observed that n-Ag: MoO_3/p-Si diodes have lower ideality factor and higher barrier height when compared to n- MoO_3/p-Si. In addition, the Silver ion substitution into MoO_3 lattice reduces the number of oxygen vacancies and leads to lower density of free carriers, which can effectively increase the barrier height at the interface.

6. CONCLUSION

Summing up, we report the successful coated of (MoO_3) thin films with Ag concentrations 1, 3 and 5 Wt.% on to the silica substrate calcined at 450 ℃ by a facile, rapid, cost effective and a custom-made Jet Nebulizer Spray Pyrolysis Technique. The concentration impact on the structural, morphological and compositional parameters of the fabricated films were examined. The structural analysis (XRD peak profile) reports the presence of orthorhombic phase of MoO_3 in the prepared sample with preferential orientation at (110), (002) and (011) planes respectively. Morphologies of the fabricated samples resembling nano structured rods were seen in FESEM images. The wide spread distribution of a crack free homogeneous surface reveals the good adhesion of the deposited films on to the silica substrates. EDX spectra confirms the presence of the elements such as Oxygen (O) Molybdenum (Mo) and Silver (Ag) in the fabricated samples. The ideality factor (4.0975) and barrier height (0.57694 eV) was obtained for 5 wt% of Ag doped MoO_3 prepared sample.

7. REFERENCES

[1]. A.I. Hassan, and S.I. Maki, *Energy Procedia.,* **119**, 961(2017); https://doi.org/10.1016/j.egypro.2017.07.129

[2] W.Li, J.Shi, Kelvin H.L.Zhang, and L.MacManus-Driscoll, *Mater.Horiz.,* **7,** 2832 (2020); https://doi.org/10.1039/D0MH00899K

[3] X.W. Lou, and H.C. Zeng, *Chem. Mater.,* **14,** 4781 (2002); https://doi.org/10.1021/cm0206237

[4] I.Alves de Castro, R.S.Datta, J.Z.Ou, A.Castellanos-Gomez, S.Sriram, T.Daeneke, and K.Kalantar-zadeh, *Adv.Mater.,* **29,** 1701619 (2017); https://doi.org/10.1002/adma.201701619

[5] T.V. Sviridova, L.Yu Sadovskaya, E.M. Shchukina, A.S. Logvinoyich, D.G. Shchukin, and D.V. Sviridov, *J.Photochem. Photochem. Photobiol. A: Chemistry.,* **327,** 44 (2016); https://doi.org/10.1016/j.jphotochem.2016.04.018

[6] T.Nagyne-Kovacs, L.Studnicks, I.E.Lukacs, K.Laszlo,P.Pasierb, I.M.Szilagyi, and G.Pokol, *Nanomaterials.,* **10,** 891 (2020); https://doi.org/10.3390/nano10050891

[7] T.A. Tran, K. Krishnamoorthy, Y.W. Song, S.K. Cho, and S.J. Kim, *ACS Appl. Mater. Interfaces.,* **6(4),** 2980 (2014); https://doi.org/10.1021/am4058586d

[8] T. Waters, R.A. O'Hair, and A.G. Wedd, *J. Am. Chem. Soc.,* **125,** 3384 (2003); https://doi.org/10.1021/ja028839x

[9] L. Zhang, G. Wu, F. Gu, and H. Zeng, *Scientific reports.,* **5,** 17388 (2015); https://doi.org/10.1038/srep17388

[10] W. Seiler, E. Million, J. Perriere, R. Benzerga, and C. Boulmer-Leborgne, *J. Cryst. Growth.,* **311,** 3352 (2009); https://doi.org/10.1016/j/jcrysgro.2009.03.047

[11] L.Boudaoud, N.Benramdance, A.Bouzidi, A.Nekerala, and R.Desfeux, *Optik.,* **127,** 852 (2016); https://doi.org/10.1016/j.ijleo.2015.10.105

[12] C.R. Dhas, A. Dinu, A.J. Christy, K. Jevadheepan, A.M.E. Raj, and C. Sanjeeviraja, *Asian J. Appl. Sci.,* **7,** 671 (2014); https://doi.org/10.3923/ajaps.2014.671.684

[13] K. Ravichandran, A. Manivasaham, K. Subha, A. Chandra Bose, and R. Muniappan, S*urf. Interfaces.,* **1-3,** 13 (2016); https://doi.org/10.1016/j.surfin.2016.06.004

[14] N. Guru Prakash, M. Dhananjaya, A.Lakshmi Narayana, H. Maseed, V.V.S.S. Srikanth, and O.M. Hussain, *Appl. Phys. A.,* **125,** 488 (2019); https://doi.org/10.1007/s00339-019-2779-2

[15] A. Klinbumrung, T. Thongtem, and S. Thongtem, *Journal of Nanomaterials.,* **40,** 1 (2012). https://doi.org/10.1155/2012/930763

[16] G.Pradeep, V.Ponnuswamy, B.Gowtham, R.Suresh, and J.Chandrasekaran, *Optik.,* **175,** 217 (2018); https://doi.org/10.1016/jijleo.2018.09.020

[17] T.H.Chiang, and H.Che Yeh, *Materials.,* **6,** 4609 (2013); https://doi.org/10.3390/ma6104609

[18] N. Rajiv Chandar, S. Agilan, R. Thangarasu, N. Muthukumarasamy, and R. Ganesh, *J Mater Sci: Mater Electron.,* **31,** 7378 (2020); https://doi.org/10.1007/s10854-019-02820-w
[19] S.Patnaik, G.Swain, and K.M.Parida, *Nanoscale.,* **10,** 5950 (2018). https://doi.org/10.1039/C7NR09049H
[20] J.V.B. Moura, J.V. Silveira, J.G. da Silva Filho, A.G. Souza Filho, C. Luz Lima, and P.T.C. Freire, *Vib. Spectosc.,* **98,** 98 (2018); https://doi.org/10.1016/j.vibspec.2018.07.008
[21] R.Sharma, R.Jha, A.Sarkar, A.K.Sharma, D.Sharma, M.Bhushan, and R.Bhardwaj, *Ceram. Int.,* **46,** 23084 (2020); https://doi.org/10.1016/j.ceramint.2020.06.085
[22] A.E.X. Gavim, M.R. Pereira da chanha, E.R. Spada, T.N. Machado, F.S. Hadano, A.G. Bezerra Jr, W.H. Schreiner, P.C. Rodrigues, A.R.B. Mohd Yusoff, A.G. Macedo, R.M. Faria, and W.J. da silva, *Energy Mater. Sol. Cells.,* **200,** (2019) 109986. https://doi.org/10.1016/j.solmat.2019.109986
[23] A.Boukhachem, O.kamoun, C.Mrabet, C.Mannai, N.Zouaghi, A.Yumak, K.Boubaker, and M.Amlouk, *Mater. Res. Bull.,* **72,** 252 (2015); https://doi.org/10.1016/j.materresbull.2015.08.011
[24] H.Hu, C.Deng, J.Xu, K.Zhange, and M.Sun, *J.Exp.Nanosci.,* **10,** 1336 (2015); https://doi.org/10.1080/17458080.2015.1012654
[25] N.Illyaskutty, S.Sreedhar, G. Sanal kumar, H.Kohler, M.Schwotzer, C.Natzeck, and V.P.M.Pillai, *Nanoscale.,* **6,** 13882 (2014); https://doi.org/10.1039/C4NR04529G
[26] N.Benameur, M.A.Chakhoum, A.Boukhachem, M.A.Dahamni, M.Ghamnia, N.Hacini, J.P.Pireaux, L.Houssiau, and A.Ziouche, *J.Electron Spect Rel Phen.ens.,* **234,** 71 (2019); https://doi.org/10.1016/j.ELSPEC.2019.05.015.

DOI: https://doi.org/10.15379/ijmst.v10i2.2902